Nonlinear Feedback Control of a Spinning Two-Spacecraft Coulomb Virtual Structure

Shuquan Wang and Hanspeter Schaub

Simulated Reprint from

IEEE Transactions on Aerospace and Electronic Systems

Vol. 47, No. 3, July 2011, pp. 2055–2067

Nonlinear Feedback Control of a Spinning Two-Spacecraft Coulomb Virtual Structure

Shuquan Wang, and Hanspeter Schaub

***Abstract*—This paper studies a spinning two-spacecraft Coulomb virtual structure control scenario in an orbital environment. Only Coulomb forces are utilized to control the two-spacecraft formation shape while flying in a geostationary orbit. After deriving the separation distance equation of motion which determines the 2-vehicle formation shape, a feed-forward nominal control charge is developed by assuming a purely two spacecraft configuration. An asymptotically stable full-state feedback control law is developed. It requires the inertial and relative position vectors which are difficult to measure accurately. A partial-state feedback control law is proven to be stable assuming a fast spinning rate in comparison to the orbit rate. The boundaries of the orbital motion contributions are proven to be negligible for a relatively tight and fast-spinning formation in a geostationary orbit. An integral feedback term is utilized to compensate for the error in estimating the feed-forward nominal charge product. Numerical simulations illustrate the performance of the controllers.**

***Index Terms*—Electrostatic spacecraft, formation flying, nonlinear control**

I. Introduction

COULOMB Formation Flying (CFF) is a novel relative motion control concept that was first introduced by Lion B. King in 2002[1]. CFF uses only the electrostatic forces (Coulomb forces) to control the shape and size of the formation of free-flying spacecraft. Earlier work in 1966 also discusses the use of Coulomb forces to electrostatically inflate a rigidly supported membrane sail structure.[2] However, here the Coulomb forces are only used to deflect the membrane, and not to actuate free-flying spacecraft. In both cases the spacecraft charges are actively controlled by continuously emitting charged particles such as electrons and ions. In a vacuum the magnitude of the Coulomb forces are inversely proportional to the square of the separation distances. Thus Coulomb forces are proposed to control a tight formation with separation distances within 100 meters.

Other novel techniques for close proximity flying include Electric Propulsion (EP)[1] and Electro-Magnetic Formation Flying (EMFF)[3]. The EP thrusting is achieved through the momentum exchange with the expelled particles. It generates high velocity, large volume (compared to Coulomb thrusting method) ionic plumes to gain a momentum in the inverse direction of the exhaust. These ionic plumes may disturb the sensors of neighboring spacecraft if the exhaust plumes impinge on them. The EMFF method creates electromagnetic dipoles on each spacecraft to generate inter-spacecraft control forces and torques. Reaction wheels are employed to orient the electromagnetic spacecraft and the associate magnetic field, and to absorb momentum imparted onto the spacecraft through the magnetic fields and torques of the other electromagnetic spacecraft. Reference [4] provides a survey of spacecraft formation flying control. Here the control strategy must consider the long term influence of differential gravity[5] or J_2 gravitational perturbations[6] to provide a fuel efficient solutions. In contrast, the CFF methods cannot achieve the kilometer level separation distances of formations using inertial thrusting, but they can provide essentially propellantless methods of direct relative motion actuation for close proximity operations.

The CFF concept is appealing in close proximity flying because of three reasons. First, using the CFF concept to control the relative motion electrostatically is essentially propellantless. The generation of the Coulomb forces is achievable with effective fuel efficiencies I_{sp} ranging from 10^9–10^{13} seconds.[1] Second, it is 3–5 orders of magnitude more power-efficient than EP.[1] It requires only several Watts of electric power to operate and can be controlled on a millisecond's time scale.[7] Third, it does not generate caustic plumes that may cause damages to some sensitive instruments during a long-term space mission. These three advantages make CFF attractive for long-term space missions.

Utilizing CFF also has some challenges. First, unlike the conventional thrusters that can produce a force vector in any direction, the Coulomb forces only lie primarily along the line-of-sight directions between spacecraft. It's very challenging to control the inertial orientation of a formation using only Coulomb forces. But the use of Coulomb forces is still attractive in controlling the relative motion between spacecraft in a formation. Second, the plasma environment in space will partially shield the electrostatic charges. This plasma shielding effect reduces the magnitude of the Coulomb force that a neighboring charged spacecraft experiences. The amount of shielding is characterized by the Debye length as discussed in References [8] and [9]. The Coulomb force magnitude drops substantially when the separation distance is greater the local Debye length. The plasma shielding effect is very strong in LEO orbit with the Debye length as small as centimeters. At GEO the Debye length ranges between 100–1000 meters.[1], [10] At 1 AU in deep space, the Debye length ranges around 20–50 meters.[1] Thus, the Coulomb thrusting concept is feasible for HEO and deep space formation missions.

Many mission scenarios utilizing CFF have been studied. Berrymann and Vasavada et al. research equilibrium charges

Graduate Research Assistant, Aerospace Engineering Sciences Department, University of Colorado at Boulder, AIAA student member, shuquan.wang@colorado.edu.

Associate Professor, Aerospace Engineering Sciences Department, University of Colorado at Boulder, AIAA Associate Fellow.

and positions for multi-satellite charged static virtual structures in References [11], [12], [13], [14]. Natarajan et al. investigate the two-craft nadir Coulomb tether control problem in References [15], [16], [17], [18] where only linearized relative motion is considered. Schaub and Hussein study the stability of a spinning two-craft Coulomb-tether in Reference [19] where the system is assumed to be in deep space and not orbiting a planet. The same authors develop a feedback control law for a three-craft collinear Coulomb tether structure in Reference [20] where the system is also assumed to be in deep space. Reference [21] develops a nonlinear control for the one-dimensional constraint three-craft Coulomb virtual structure.

The above works are directly related to the control of a Coulomb virtual structure. Other than the above works, Joe et al. introduce a formation coordinate frame which tracks the principal axes of the formation in Reference [22]. Lappas et al. in Reference [23] develop a hybrid propulsion strategy to control the relative motion of a cluster of spacecraft by combining Coulomb forces and standard electric thrusters for formation flying on the orders of tens of meters in GEO. Simulation results show that incorporating the Coulomb forces into the hybrid control of a spacecraft cluster can yield more than 80% saving in power for propulsion. Reference [24] proposes a N-craft Coulomb structure control strategy by utilizing three drone spacecraft to assist controlling the N main spacecraft. References [25] and [26] study the instantaneous 2-spacecraft collision avoidance control problem.

This paper investigates the nonlinear control of a spinning two-craft Coulomb virtual structure orbiting the Earth at a geostationary orbit. A Coulomb virtual structure is a cluster/formation of spacecraft controlled by only Coulomb forces to establish a certain fixed configuration. A two-craft Coulomb virtual structure is the simplest case of general Coulomb virtual structure control problems. But the study of the two-craft control provides fundamental insights to general Coulomb virtual structure control problem. Because the charges appear in a nonlinear and coupled form in the equations of motion, the control problem quickly becomes excessively challenging when the number of the spacecraft is greater than two. Thus fully understanding the two-craft Coulomb virtual structure control is a good foundation for studying the general Coulomb virtual structure control problem.

Note that if the two-craft system is rotating at the same rate as the orbital period, then charged relative equilibrium configurations are possible. Here the two satellites are frozen relative to the local Hill frame as discussed in Reference [12]. Earlier active feedback control work in References [15] and [16] on the control of a charged two-craft system only considers linearized motion about these special relative equilibria where spin and orbit rates are matched. In contrast, this paper investigates a nonlinear control strategy which can stabilize a spinning two-craft system which is in orbit. Unlike the two-craft spinning system discussed in Reference [19], which is passively stable if the separation distance is less than the local Debye length, when orbiting a planet the differential gravity will cause the spinning two-craft system to be unstable without feedback. The paper investigates the requirement for full-state measurements to achieve shape convergence, as well as how simpler reduced state measurements can be used to still guarantee a stable system. The relative position vectors can be challenging to measure accurately for a close proximity formation. Here the three-dimensional shape and orientation of the formation objects must be taken into account when using optical or radio-wave signals to determine relative motion. Alternatively, dropping these position vector feedback terms may introduce errors of the control. This paper studies the influence of dropping the position vector feedback terms. Numerical simulations are used to illustrate the resulting feedback control law performance.

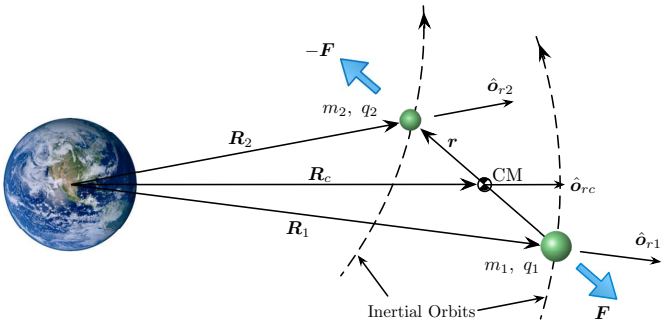

Fig. 1. Scenario of the 2 spacecraft system.

II. Equations Of Motion

This paper considers a scenario where a two-spacecraft formation operates in a Geostationary Earth Orbit (GEO). The actively controlled electrostatic forces (Coulomb forces) between the spacecraft are the sole method utilized to control the separation distance. No hybrid thrusting is considered. Note that Coulomb forces cannot directly change the inertial angular momentum of the system because they are system-internal forces. Instead, the objective of the control is to maintain the separation distance to be a certain desired value such that the shape of the two-body formation is held.

Assuming the spacecraft potential is small compared to the local plasma kinetic energy, the Coulomb force between the two spacecraft acting on spacecraft-1 (SC-1) is approximated as[26]:

$$\boldsymbol{F}_c = -k_c \frac{Q}{L^2}\left(1+\frac{L}{\lambda_{\rm d}}\right) e^{-\frac{L}{\lambda_{\rm d}}} \hat{\boldsymbol{e}}_r \tag{1}$$

where $k_c = 8.99 \times 10^9\ \mathrm{Nm^2C^{-2}}$ is the Coulomb constant, Q is the charge product of the two spacecraft, $L = \|\boldsymbol{r}\|$ is the separation distance between the two spacecraft, $\hat{\boldsymbol{e}}_r = \boldsymbol{r}/L$ is the unit vector pointing from SC-1 to SC-2, $\lambda_{\rm d}$ is the Debye length characterizing the plasma shielding effect.

The inertial equations of motion (EOM) are given by

$$m_1 \ddot{\boldsymbol{R}}_1 = -\frac{GMm_1}{R_1^2}\hat{\boldsymbol{o}}_{r1} - k_c \frac{Q}{L^2}\left(1+\frac{L}{\lambda_{\rm d}}\right) e^{-\frac{L}{\lambda_{\rm d}}} \hat{\boldsymbol{e}}_r \tag{2a}$$

$$m_2 \ddot{\boldsymbol{R}}_2 = -\frac{GMm_2}{R_2^2}\hat{\boldsymbol{o}}_{r2} + k_c \frac{Q}{L^2}\left(1+\frac{L}{\lambda_{\rm d}}\right) e^{-\frac{L}{\lambda_{\rm d}}} \hat{\boldsymbol{e}}_r \tag{2b}$$

where $G = 6.67428 \times 10^{-11}\ \mathrm{m^3kg^{-1}s^{-2}}$ is the gravitational constant, $M = 5.9736 \times 10^{24}$ kg is the Earth's mass. The

states $\boldsymbol{R}_i$, m_i and q_i are the inertial position vector, the mass and the charge of the i^{th} spacecraft respectively, while $\hat{\boldsymbol{o}}_{ri} = \boldsymbol{R}_i/L_i$ is the unit vector of the inertial position vector of the i^{th} spacecraft.

In order to develop a control algorithm to stabilize the separation distance (i.e. the virtual structure shape) of the two spacecraft, we derive the separation distance equation of motion.Using Eq. (2), the relative EOM is:

$$\begin{aligned}\ddot{\boldsymbol{r}} =&\ddot{\boldsymbol{R}}_2 - \ddot{\boldsymbol{R}}_1 = \frac{GM}{R_1^2}\hat{\boldsymbol{o}}_{r1} - \frac{GM}{R_2^2}\hat{\boldsymbol{o}}_{r2} \\ &+ k_c\frac{Q}{L^2}\left(\frac{1}{m_1}+\frac{1}{m_2}\right)\left(1+\frac{L}{\lambda_d}\right)e^{-\frac{L}{\lambda_d}}\hat{\boldsymbol{e}}_r \end{aligned} \tag{3}$$

Differentiating the identity $L = \boldsymbol{r}\cdot\hat{\boldsymbol{e}}_r$ twice yields the separation distance acceleration relationship:

$$\ddot{L} = \ddot{\boldsymbol{r}}\cdot\hat{\boldsymbol{e}}_r + \frac{1}{L}\|\dot{\boldsymbol{r}}\|^2\Big(1-\cos^2\angle(\boldsymbol{r},\ \dot{\boldsymbol{r}})\Big) \tag{4}$$

Substituting Eq. (3) into Eq. (4) yields the desired separation distance EOM:

$$\begin{aligned}\ddot{L} =&k_c\frac{Q}{L^2}\left(\frac{1}{m_1}+\frac{1}{m_2}\right)\left(1+\frac{L}{\lambda_d}\right)e^{-\frac{L}{\lambda_d}} \\ &+\underbrace{GM\left(\frac{1}{R_1^2}\hat{\boldsymbol{o}}_{r1}-\frac{1}{R_2^2}\hat{\boldsymbol{o}}_{r2}\right)\cdot\hat{\boldsymbol{e}}_r}_{f_1} \\ &+\underbrace{\frac{1}{L}\|\dot{\boldsymbol{r}}\|^2\Big(1-\cos^2\angle(\boldsymbol{r},\ \dot{\boldsymbol{r}})\Big)}_{f_2}\end{aligned} \tag{5}$$

Note that the term f_1 is the projection of the relative acceleration due to gravity along the relative position direction and is a function of the inertial position vectors of the formation. In contrast, f_2 is solely a function of the relative position vectors of the formation.

III. Two-Craft Shape Control Algorithm

The goal of this paper is to develop a static shape control of a spinning charged two-spacecraft formation. The control objective is thus only the shape of the formation, not the orientation of the formation. This section develops a Lyapunov-based nonlinear controller to make the separation distance of the two spacecraft stabilized at the desired distance. Let us define a shape error as

$$\Delta x = L - L^* \tag{6}$$

where L^* is the desired constant distance. The objective of the control is to make $\Delta x \to 0$. Because the desired distance L^* is constant, the relative trajectory of the two body system is circular. For a two body Coulomb formation with separation distance within 100m, the satellites' major accelerations is due to the Coulomb forces. Thus, after the distance error converges, the control charge would be a constant value that maintains the shape of the spinning structure. This paper defines the control charge product as a summation of a feed-forward and a feedback component:

$$Q = Q_n + \delta Q \tag{7}$$

Here Q_n is the feed-forward control component that maintains the shape of the final spinning structure, δQ is the feedback part that stabilizes the distance error.

A. Spinning Two-Craft Feed-Forward Control

The feed-forward control is obtained by finding the equilibrium solution of the control charge product under the assumption that the two spacecraft are flying in deep space. This way the influence of the planetary gravity is treated as a disturbance that is taken care of by the feedback control component. Neglecting the planetary gravity influences, the EOM in Eq. (5) becomes

$$\ddot{L}^* = k_c\frac{Q}{L^{*2}}\left(\frac{1}{m_1}+\frac{1}{m_2}\right)\left(1+\frac{L^*}{\lambda_d}\right)e^{-\frac{L^*}{\lambda_d}} + f_2^* \tag{8}$$

where f_2^* is the ideal value of f_2 when the distance error converges to zero. Forcing $\ddot{L} = 0$ yields the feed-forward control charge product:

$$Q_n = -\frac{L^{*2}\lambda_d}{k_c(L^*+\lambda_d)}\frac{m_1m_2}{m_1+m_2}e^{\frac{L^*}{\lambda_d}}f_2^* \tag{9}$$

Note that Q_n is a constant, it does not compensate for the distance error Δx. When implementing the feed-forward control, an estimated value of f_2^* is required at the beginning of the control.

Note that to obtain an estimate f_2^*, measurements of both $\boldsymbol{r}$ and $\dot{\boldsymbol{r}}$ are required at an instant. If the accuracy requirement of these measurements can be reduced, or the requirement for f_2^* removed, then this charge control would be much simpler to implement.

B. Full-State Feedback Control & Stability Analysis

The prior section determines the feed-forward charge product for a circular relative orbit by assuming a pure two-spacecraft system. This section develops the charge feedback component of the final control that stabilizes the shape errors.

Define a Lyapunov candidate function as

$$V(\Delta x, \Delta\dot{x}) = \frac{1}{2}p\Delta x^2 + \frac{1}{2}\Delta\dot{x}^2 \tag{10}$$

Taking a time derivative of V yields:

$$\begin{aligned}\dot{V} =&\Delta\dot{x}(p\Delta x + \Delta\ddot{x}) \\ =&\Delta\dot{x}\Bigg(k\Delta x + f_1 + f_2 \\ &+ k_c\frac{Q}{L^2}\left(\frac{1}{m_1}+\frac{1}{m_2}\right)\left(1+\frac{L}{\lambda_d}\right)e^{-\frac{L}{\lambda_d}}\Bigg)\end{aligned} \tag{11}$$

Ideally we would like to force $\dot{V}$ to be of the following negative semi-definite form:

$$\dot{V}(\Delta x, \Delta\dot{x}) \triangleq -d\Delta\dot{x}^2 \tag{12}$$

with $d > 0$. Note that $\dot{V}$ is negative semi-definite because V is a function of both Δx and $\Delta\dot{x}$, but only $\Delta\dot{x}$ appears in $\dot{V}$. Thus, $\dot{V} = 0$ if $\Delta\dot{x} = 0$ regardless of what Δx is. Studying the higher order derivatives of V, as shown by Mukherjee and

Chen in Reference [27], it can be shown that this control will be asymptotically stabilizing.

Substituting Eq. (11) into Eq. (12), and solving for the feedback charge product δQ_f, yields:

$$\delta Q_f = \frac{L^2}{k_c}\frac{m_1 m_2}{m_1+m_2}\frac{\lambda_d}{L+\lambda_d}e^{-\frac{L}{\lambda_d}}\big(-p\Delta x - d\Delta\dot{x} - f_1 - f_2 + f_2^*\big) \quad (13)$$

Note that the f_2^* term in the brackets comes from the feed-forward control Q_n in Eq. (9). The usage of this term is to cancel out the function of the relative position vector f_2. However f_2^* is a constant while f_2 is time varying, perfect canceling f_2 is not achievable. Because the f_1 function requires knowledge of the inertial position vectors of the two spacecraft, this feedback control law in Eq. (13) is called the full-state feedback controller.

The full-state feedback controller given by Eq. (13) ensures $\dot{V}$ to be negative semidefinite as shown in Eq. (12). Taking a second time derivative of V, yields

$$\ddot{V} = -2d\Delta\dot{x}\Delta\ddot{x} \quad (14)$$

When $\dot{V}=0$, $\Delta\dot{x}=0$, thus $\ddot{V}=0$. Taking a third time derivative of V, yields

$$\dddot{V} = -2d\Delta\ddot{x}^2 - 2d\Delta\dot{x}\Delta\dddot{x} \quad (15)$$

When $\dot{V}=0$, $\dddot{V} = -2d\Delta\ddot{x}^2 < 0$. Thus the system is asymptotically stable under the full-state feedback controller in Eq. (13)

C. Partial-State Feedback Control & Stability Analysis

The full-state feedback control law given by Eqs. (9) and (13) developed in the previous section requires the measurement of the inertial and relative position vectors. If the measurement is accurate then the full-state feedback control law is asymptotically stable. However, these position vectors can be challenging to measure accurately in a tight formation flying in GEO orbit with separation distance within 100m. This section studies the separation distance feedback controller with the feedback components simplified to only require separation distance measurements:

$$\delta Q_p = \frac{L^2}{k_c}\frac{m_1 m_2}{m_1+m_2}\frac{\lambda_d}{L+\lambda_d}e^{-\frac{L}{\lambda_d}}\left(-p\Delta x - d\Delta\dot{x}\right) \quad (16)$$

The feed-forward part is given by Eq. (9). The feedback part δQ_p in Eq. (16) is obtained by removing the f_1 function from δQ_f in Eq. (13). It requires only the measurement of the separation distance which is easy to measure accurately. Substituting Eqs. (9) and (16) into the EOM in Eq. (5) yields

$$\Delta\ddot{x} + d\Delta\dot{x} + p\Delta x = f_1 + f_2 - f_2^* \quad (17)$$

Note that f_2 is a function of the relative position vector and is thus time varying. Thus $f_2^* - f_2$ never stays at zero no matter what the guess of f_2^* would be. In order to study this error, let us start from the expression of f_2:

$$f_2 = \frac{1}{L}\|\dot{\boldsymbol{r}}\|^2\big(1-\cos^2\angle(\boldsymbol{r},\dot{\boldsymbol{r}})\big) \quad (18)$$

It is beneficial if f_2 can be expressed in terms of the states Δx and $\Delta\dot{x}$, allowing the Taylor series expansion to be utilized to linearize the function f_2 about the estimated value f_2^*. The following identities are used in developing new expression of f_2:

$$\begin{cases} \boldsymbol{r} = L\hat{\boldsymbol{e}}_r \\ \dot{\boldsymbol{r}} = \dot{L}\hat{\boldsymbol{e}}_r + L\dot{\theta}\hat{\boldsymbol{e}}_\theta \end{cases} \quad (19)$$

The cosine function in Eq. (18) is expressed by:

$$\cos\angle(\boldsymbol{r},\dot{\boldsymbol{r}}) = \frac{\boldsymbol{r}\cdot\dot{\boldsymbol{r}}}{\|\boldsymbol{r}\|\|\dot{\boldsymbol{r}}\|} = \frac{\dot{L}}{\sqrt{\dot{L}^2+(L\dot{\theta})^2}} \quad (20)$$

For a fast spinning two-craft formation, the momentum is approximately conserved if the local gravity gradient torque can be ignored over the short-term (fraction of an orbit):

$$h = L^2\dot{\theta} = L^{*2}\dot{\theta}^* \quad (21)$$

where L^* is the expected separation distance, $\dot{\theta}^*$ is the nominal spinning angular rate. Solving for $\dot{\theta}$ from Eq. (21) yields

$$\dot{\theta} = \frac{L^{*2}}{L^2}\dot{\theta}^* \quad (22)$$

Substituting Eq. (22) into Eq. (20) yields

$$\cos\angle(\boldsymbol{r},\dot{\boldsymbol{r}}) = \frac{\dot{L}}{\sqrt{\dot{L}^2+\left(\frac{L^{*2}}{L}\dot{\theta}^*\right)^2}} \quad (23)$$

Substituting Eqs. (19) and (23) into Eq. (18) yields

$$f_2 = \frac{L^{*4}}{L^3}\dot{\theta^*}^2 \quad (24)$$

In this expression only L is a variable, other parameters are constants determined by the expected separation distance and nominal spinning rate. Thus f_2 is a function of L by assuming a fast spinning two-craft formation compared to the orbit period. Taking a Taylor series expansion about the expected separation distance yields the first order relationship:

$$f_2(L) = f_2^* + \frac{\mathrm{d}f_2}{\mathrm{d}L}\Delta x = f_2^* - \frac{3L^{*4}}{L^4}\dot{\theta^*}^2\Delta x + O(\Delta x^2) \quad (25)$$

Substituting Eq. (25) into the close-loop EOM in Eq. (17) yields

$$\Delta\ddot{x} + d\Delta\dot{x} + p\Delta x + \frac{3h^{*2}}{L^4}\Delta x = f_1 \quad (26)$$

where $h^* = L^{*2}\dot{\theta}^*$ is the nominal momentum. Note that f_1 is a function of the inertial position vector. The next section will prove that the value of f_1 is very small for a formation in GEO orbit (the magnitude is up to 10^{-6}m/s^2), thus the influence of f_1 can be neglected for short-term stability discussions. Note that the close-loop dynamics in Eq. (26) is obtained by assuming the feed-forward part has perfect estimation $\hat{f}_2$ of the expected value f_2^*. If the estimation is not perfect, then there would exist a constant bias in the EOM. Denote the estimation error as

$$\delta f_2 = f_2^* - \hat{f}_2 \quad (27)$$

then the EOM in Eq. (26) becomes

$$\Delta\ddot{x} + d\Delta\dot{x} + \left(p + \frac{3h^{*2}}{L^4}\right)\Delta x = \delta f_2 \tag{28}$$

The estimation error δf_2 acts as a constant perturbation to the system and may introduce bias or even destroy the stability of the system. To get rid of this constant error, this paper inserts an integral feedback term in the feedback control component:

$$\delta Q_{p2} = \frac{L^2}{k_c}\frac{m_1 m_2}{m_1+m_2}\frac{\lambda_d}{L+\lambda_d}e^{-\frac{L}{\lambda_d}}\Big(-p\Delta x - d\Delta\dot{x} - k_i\int\Delta x\Big) \tag{29}$$

By assuming a fast spinning two-craft formation and ignoring the inertial position function f_1, the partial-state feedback control law in Eq. (16) is proven to be stable. If there is an error of the estimated value of the expected f_2^* function, there would be a constant perturbation to the system that may introduce bias or instability factor. A new feedback controller that includes an integral feedback is used to get rid of the constant bias. But the stability has not been analytically proved yet.

Schaub et. al. study the spinning 2-craft formation in Reference [19]. They prove that the 2-craft spinning Coulomb tether is passively stable in deep space. This paper considers a different situation where the 2-craft system is spinning in a GEO orbit. The gravitation forces are treated as additional disturbances. The stability is ensured for short term fast spin compared to the orbit rate. But long term stability is not ensured.

D. Boundaries of the f_1 function

The previous section develops an asymptotically stable full-state feedback controller and a stable partial-state feedback controller. The stability proof of the partial-state feedback controller assumes the influence of the inertial position function f_1 is negligible. This section investigates the boundaries of the function f_2.

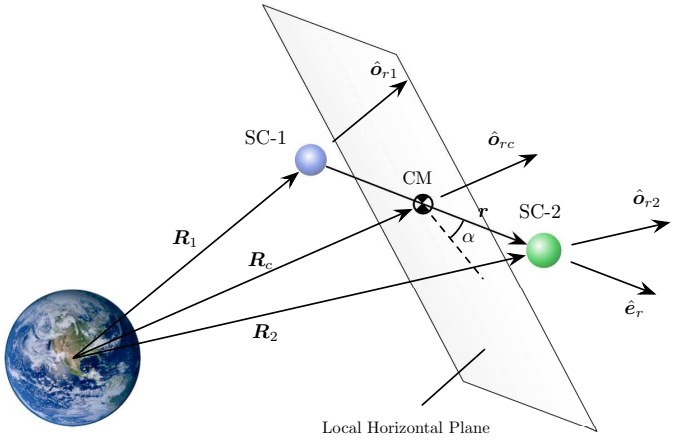

Fig. 2. Geometry of a generally rotating 2-craft system in Earth Orbit.

Let us start from the definition of f_1:

$$f_1 = \frac{GM}{R_1^2}\hat{\boldsymbol{o}}_{r1}\cdot\hat{\boldsymbol{e}}_r - \frac{GM}{R_2^2}\hat{\boldsymbol{o}}_{r2}\cdot\hat{\boldsymbol{e}}_r \tag{30}$$

Because CFF considers formation with separation distance within 100 meters, L is very small comparing with R_i. The following approximations have sufficient accuracy (the error is within 3×10^{-5}m for the formation in GEO orbit):

$$R_1 = R_c - \frac{1}{2}L\sin\alpha \tag{31a}$$

$$R_2 = R_c + \frac{1}{2}L\sin\alpha \tag{31b}$$

where α is the angle between the unit vector $\hat{\boldsymbol{e}}_r$ and the local horizon plane as shown in Figure 2. The angle α values are within $[-90,\ 90]^{\circ}$. From Figure 2, the unit vectors $\hat{\boldsymbol{o}}_{r1}$ and $\hat{\boldsymbol{o}}_{r2}$ are expressed as

$$\hat{\boldsymbol{o}}_{r1} = \frac{1}{R_1}(R_c\hat{\boldsymbol{o}}_{rc} - \frac{1}{2}L\hat{\boldsymbol{e}}_r) \tag{32a}$$

$$\hat{\boldsymbol{o}}_{r2} = \frac{1}{R_2}(R_c\hat{\boldsymbol{o}}_{rc} + \frac{1}{2}L\hat{\boldsymbol{e}}_r) \tag{32b}$$

Substituting Eq. (31) and Eq. (32) into Eq. (30), yields:

$$\begin{aligned} f_1 =& GM\left(\frac{R_c\hat{\boldsymbol{o}}_{rc}\cdot\hat{\boldsymbol{e}}_r - 0.5L}{(R_c - 0.5L\sin\alpha)^3} - \frac{R_c\hat{\boldsymbol{o}}_{rc}\cdot\hat{\boldsymbol{e}}_r + 0.5L}{(R_c + 0.5L\sin\alpha)^3}\right) \\ =& GM\left(\frac{R_c\sin\alpha - 0.5L}{(R_c - 0.5L\sin\alpha)^3} - \frac{R_c\sin\alpha + 0.5L}{(R_c + 0.5L\sin\alpha)^3}\right) \end{aligned} \tag{33}$$

Now the term f_1 has been expressed as a function of the center of mass (CM) radius R_c, the separation distance L and the angle α. Note that this paper considers a short-distance formation in a GEO orbit, the CM radius can be approximated by the radius of the GEO orbit $R_c = 4.2155\times10^7$m. The separation distance is within 100 meters, at the steady state it is close to the desired value. The angle α can not be controlled because Coulomb forces are internal forces in the formation and are not capable to directly control the inertial orientation of the formation. The angle α is the most rapidly varying quanity in the expression of f_1 in Eq. (33), and it is the only variable when the formation is at the steady state. The behavior of f_1 when α is changing should be identified.

Taking a partial derivative of f_1 with respect to (w.r.t.) α, yields:

$$\begin{aligned} \frac{\partial f_1}{\partial\alpha} = GM\Bigg\{&\frac{1}{\rho_1^4}\Big(R_c^2\cos\alpha + R_cL\sin\alpha\cos\alpha - 0.75L^2\cos\alpha\Big) \\ &- \frac{1}{\rho_2^4}\Big(R_c^2\cos\alpha - R_cL\sin\alpha\cos\alpha - 0.75L^2\cos\alpha\Big)\Bigg\} \end{aligned} \tag{34}$$

where $\rho_1 = R_c - 0.5L\sin\alpha$ and $\rho_2 = R_c + 0.5L\sin\alpha$. The extrema occurs when $\dfrac{\partial f_1}{\partial\alpha} = 0$. From Eq. (34), one obvious solution that makes the partial derivative be zero is $\cos\alpha = 0$. When $\cos\alpha = 0$ then $\sin\alpha = \pm1$. Substituting $\sin\alpha = \pm1$ into the expression of f_1 in Eq. (33), yields:

$$f_1^{(1)} = GM\left[\frac{1}{(R_c - 0.5L)^2} - \frac{1}{(R_c + 0.5L)^2}\right] \tag{35}$$

Another solution that makes the partial derivative in Eq. (34) be zero is $\sin\alpha=0$. Substituting $\sin\alpha=0$ into Eq. (33), yields:

$$f_1^{(2)} = -\frac{GML}{R_c^3} \tag{36}$$

The following theorem proves that $f_1^{(1)}$ is the maximum of f_1, and $f_1^{(2)}$ is the minimum of f_1.

Theorem 1: Given a function of α defined by Eq. (33). Assume that L is constant and $\alpha \in [-90,\ 90]^{\circ}$. If $R_c \gg L$, then the maximum value occurs when $\cos\alpha=0$, the minimum value occurs when $\sin\alpha=0$. The maximum value is $f_1^{(1)}$ given by Eq. (35) and the minimum value is given by Eq. (36).

Proof: The derivation from Eq. (34) to Eq. (36) has proven that $f_1^{(1)}$ and $f_1^{(2)}$ are two extrema of the function f_1. Further investigation is needed to show that these two extrema a lower and upper bound of the function f_1. Taking a second order partial derivative of f_1 w.r.t. α, yields:

$$\begin{aligned}\frac{\partial^2 f_1}{\partial\alpha^2} = GM\Bigg\{ & \\ \frac{1}{\rho_1^4}\big(&-R_c^2\sin\alpha + R_cL\cos^2\alpha - R_cL\sin^2\alpha + 0.75L^2\sin\alpha\big) \\ &+ \frac{2L\cos\alpha}{\rho_1^5}\big(R_c^2\cos\alpha + R_cL\sin\alpha\cos\alpha - 0.75L^2\cos\alpha\big) \\ -\frac{1}{\rho_2^4}\big(&-R_c^2\sin\alpha - R_cL\cos^2\alpha - R_cL\sin^2\alpha + 0.75L^2\sin\alpha\big) \\ &+ \frac{2L\cos\alpha}{\rho_2^5}\big(R_c^2\cos\alpha - R_cL\sin\alpha\cos\alpha - 0.75L^2\cos\alpha\big)\Bigg\}\end{aligned} \tag{37}$$

When $\cos\alpha=0$ and $\sin\alpha=1$, $\alpha=\dfrac{\pi}{2}$. The second order partial derivative becomes:

$$\begin{aligned}\left.\frac{\partial^2 f_1}{\partial\alpha^2}\right|_{\alpha=90^{\circ}} = GM\Bigg\{&(-R_c^2+0.75L^2) \\ &\left(\frac{1}{(R_c-0.5L)^4} - \frac{1}{(R_c+0.5L)^4}\right) \\ &- R_cL\left(\frac{1}{(R_c-0.5L)^4} + \frac{1}{(R_c+0.5L)^4}\right)\Bigg\}\end{aligned} \tag{38}$$

Because $R_c \gg L$, $(-R_c^2+0.75L^2) < 0$. The following inequality is evident:

$$\frac{1}{(R_c-0.5L)^4} - \frac{1}{(R_c+0.5L)^4} > 0 \tag{39}$$

So the value of the second partial derivative in Eq. (38) is negative:

$$\left.\frac{\partial^2 f_1}{\partial\alpha^2}\right|_{\alpha=90^{\circ}} < 0 \tag{40}$$

When $\cos\alpha=0$ and $\sin\alpha=-1$, $\alpha=-\dfrac{\pi}{2}$. Then the second order partial derivative is:

$$\begin{aligned}\left.\frac{\partial^2 f_1}{\partial\alpha^2}\right|_{\alpha=-90^{\circ}} = GM\Bigg\{&\\ &(R_c^2-0.75L^2)\left(\frac{1}{(R_c+0.5L)^4} - \frac{1}{(R_c-0.5L)^4}\right) \\ &- R_cL\left(\frac{1}{(R_c+0.5L)^4} + \frac{1}{(R_c-0.5L)^4}\right)\Bigg\}\end{aligned} \tag{41}$$

Note that

$$\frac{1}{(R_c+0.5L)^4} - \frac{1}{(R_c-0.5L)^4} < 0 \tag{42}$$

So the partial derivative in Eq. (41) is negative:

$$\left.\frac{\partial^2 f_1}{\partial\alpha^2}\right|_{\alpha=-90^{\circ}} < 0 \tag{43}$$

From the two results in Eqs. (40), (43), it can be concluded that $\cos\alpha=0$ is the maximum point of the f_1 function. This proves that $f_1^{(1)}$ is the maximum value of f_1.

When $\sin\alpha=0$, $\alpha=0$. The second order partial derivative is

$$\left.\frac{\partial^2 f_1}{\partial\alpha^2}\right|_{\alpha=0} = GM\left\{\frac{2R_cL}{R_c^4} + \frac{4L}{R_c^5}\big(R_c^2-0.75L^2\big)\right\} \tag{44}$$

Clearly each term in Eq. (44) is positive, so the partial derivative in Eq. (44) is positive

$$\left.\frac{\partial^2 f_1}{\partial\alpha^2}\right|_{\alpha=0} > 0 \tag{45}$$

This indicates that $f_1^{(2)}$ in Eq. (36) is the minimum value of the function f_1. ■

Theorem 1 proves that $f_1^{(1)}$ and $f_1^{(2)}$ are upper and lower bounds of the function f_1. Thus the value level of f_1 can be determined by these two boundaries. For a formation flying in a GEO orbit with separation distance within 100m, the boundaries for $f_1^{(1)}$ and $f_1^{(2)}$ are determined:

$$f_1^{(1)} \leq 1.0646\times10^{-6}\text{m/s}^2 \tag{46}$$

$$|f_1^{(2)}| \leq 5.3228\times10^{-7}\text{m/s}^2 \tag{47}$$

Figure 3 shows the real values and boundaries of f_1 and f_2 in a simulation test. Figures 3(a) and 3(b) show the distance error history and the control charge product history. After around 3000s the distance error settles down to be close to zero. Figure 3(c) shows the boundaries of f_1. Figure 3(d) shows the true value and the estimation of the relative position feedback term f_2. Comparing with Figure 3(c), the magnitude of the function f_2 is 4 times greater in order than f_1. Thus the influence of the inertial position function f_1 can be ignored.

E. Comparison Of The Functions f_1 And f_2

The last section finds the upper and lower bounds of the function f_1 which is determined by the gravitational forces. A simulation case shows that the influence of f_1 is typically very small as compared to f_2. This section uses numerical sweeping to investigate in detail the magnitudes of f_1 and f_2 under different conditions. The results can help to determine whether

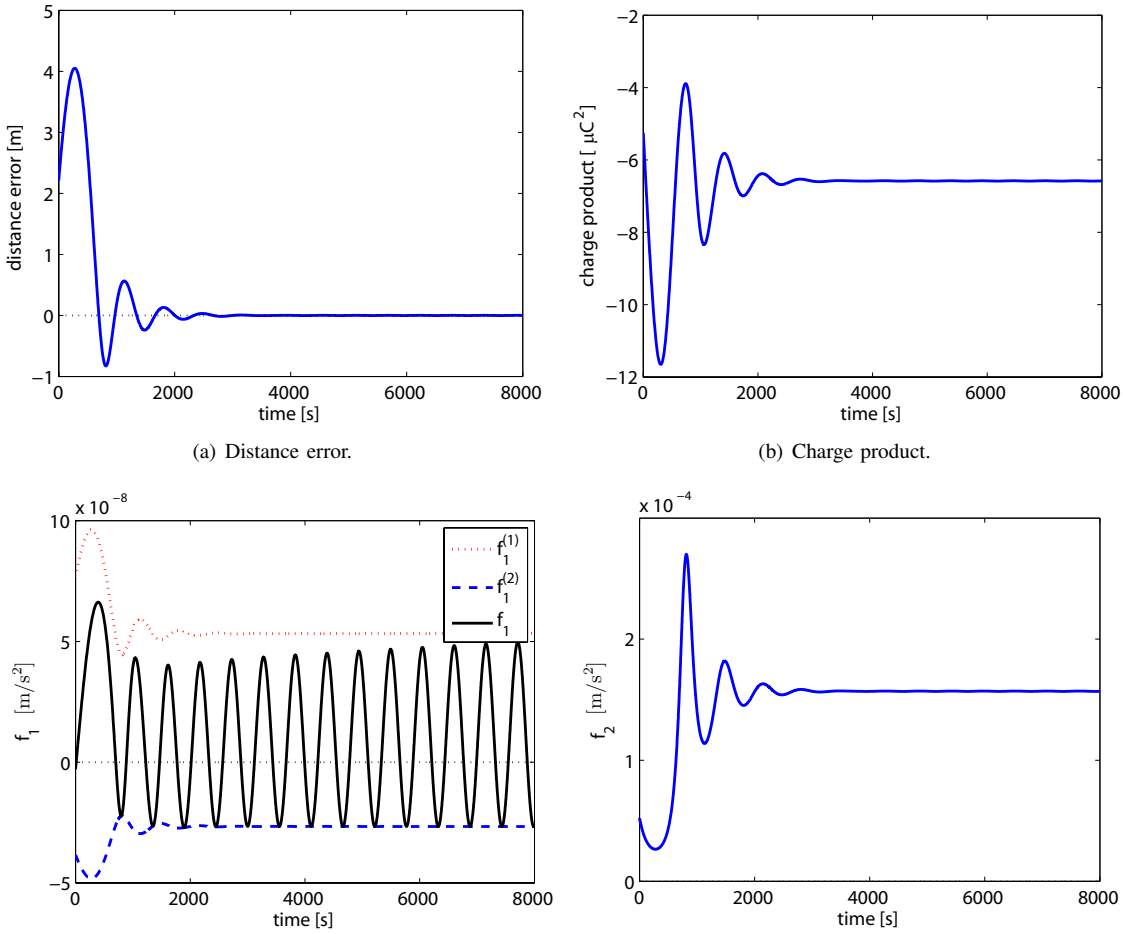

(a) Distance error.

(b) Charge product.

(c) Boundary of f_1.

(d) History of f_2.

Fig. 3. A simulation example to show the boundaries of f_1 and the history of f_2.

the gravitation influence term f_1, which requires the inertial position feedback, can be ignored under a specific condition.

By the definitions of f_1 and f_2 in Eqs. (33) and (18) respectively, these two terms are varying with the separation distance and the relative speed. Figure 4 shows the the magnitudes of f_1 and f_2 by sweeping the value of the separation distance and the relative speed. Note that the values of f_1 and f_2 are calculated assuming the spinning two-craft system is in the nominal states, which indicates that the separation distance doesn't change and the relative velocity is perpendicular to the relative position vector.

Figure 4(a) shows the magnitudes of f_1 and f_2 when sweeping the separation distance. The relative speed magnitude is set to 1cm/s. It shows that when $L < 96$, f_2 is greater than f_1. When $L < 20$m, f_2 is at least one order greater than f_1. Figure 4(b) shows the magnitudes of f_1 and f_2 when sweeping the relative speed magnitude. It shows that when $v > 0.41$cm/s, $f_2 > f_1$. f_2 increases quadratically as the speed increases, f_1 doesn't change with respect to the relative speed.

Coulomb formation flying considers very tight formation with separation distances within 100m. So from the above results, if the relative speed is at cm/s level or above, the influence of f_2 dominates and f_1 can be ignored. Otherwise the influence of dropping the inertial feedback term f_1 maybe significant and needs to be considered carefully.

IV. Numerical Simulations

A Lypunov-based nonlinear feedback control law has been developed in the previous section. The control requires only the separation distance and rate feedback. It ignores the two position vectors' functions f_1 and f_2. The boundaries of the two functions are investigated. In this section, several numerical simulations are used to test the performance of the controller and the behavior of the 2-craft formation.

The masses of the spacecraft are:

$$m_1 = m_2 = 50 \text{ kg} \tag{48}$$

The mass of the Earth is $M = 5.9742 \times 10^{24}$kg. The gravitational constant is $G = 6.67428 \times 10^{-11}\text{m}^3\text{kg}^{-1}\text{s}^{-2}$. Because the plasma shielding effect is strong at Low Earth Orbit (LEO), Coulomb formation flying considers formations in GEO or deep space. The initial position of the center of mass (CM) of the 2-craft system is set to be

$$\boldsymbol{R}_c(t_0) = [R_c,\ 0,\ 0]^T \tag{49}$$

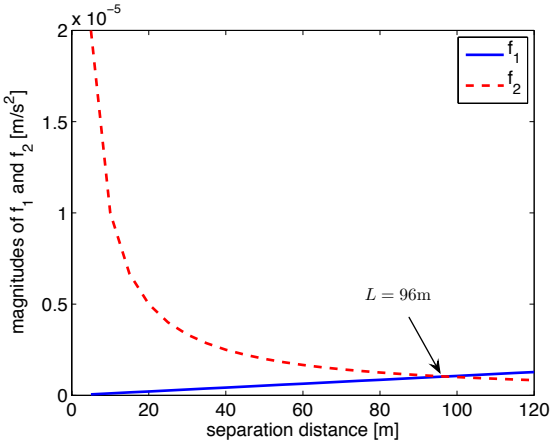

(a) Sweep L with $v = 1$cm/s.

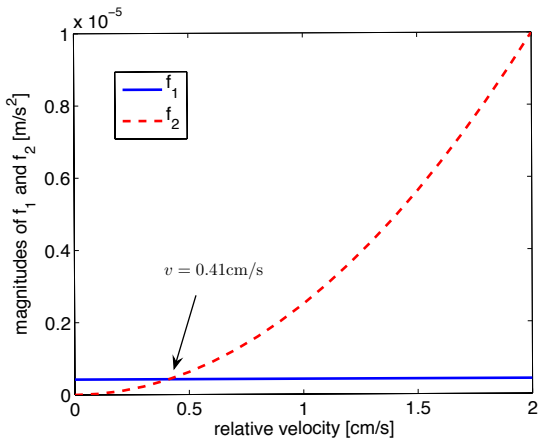

(b) Sweep v with $L = 20$m.

Fig. 4. Comparison of f_1 and f_2 under different conditions.

where $R_c = 42155000$m which is the radius of a GEO orbit. Note that the vector $\boldsymbol{R}_c(t_0)$ is expressed in the ECI frame. The initial positions of the two spacecraft are functions of $R_c(t_0)$:

$$\boldsymbol{R}_1(t_0) = \boldsymbol{R}_c(t_0) - \frac{m_2}{m_1+m_2}\boldsymbol{r}(t_0), \tag{50}$$

$$\boldsymbol{R}_2(t_0) = \boldsymbol{R}_c(t_0) + \frac{m_1}{m_1+m_2}\boldsymbol{r}(t_0). \tag{51}$$

where $\boldsymbol{r}(t_0)$ is the initial relative position vector expressed in the ECI frame. Note that the initial position of the CM $\boldsymbol{R}_c(t_0)$ and the spacecraft masses m_1 and m_2 have been determined, the initial relative position vector $\boldsymbol{r}(t_0)$ determines the initial positions of the two spacecraft. The value of the relative position vector $\boldsymbol{r}(t_0)$ will be specified in the specific simulations cases.

The initial velocity of the CM of the two spacecraft system is defined as

$$\dot{\boldsymbol{R}}_c(t_0) = [0,\ v_c, 0]^T \text{m/s} \tag{52}$$

where $v_c = 3070$m/s is the nominal speed of a GEO orbit. Corresponding to the initial positions of the two spacecraft in Eq. (50), the initial velocities of the two spacecraft are given by:

$$\dot{\boldsymbol{R}}_1(t_0) = \dot{\boldsymbol{R}}_c(t_0) - \frac{m_2}{m_1+m_2}\dot{\boldsymbol{r}}(t_0), \tag{53}$$

$$\dot{\boldsymbol{R}}_2(t_0) = \dot{\boldsymbol{R}}_c(t_0) + \frac{m_1}{m_1+m_2}\dot{\boldsymbol{r}}(t_0) \tag{54}$$

where $\dot{\boldsymbol{r}}(t_0)$ is the initial relative velocity. The value of $\dot{\boldsymbol{r}}(t_0)$ will be specified in the specific simulation cases as well.

A. Full-State Feedback Control Results

The full-state feedback control law in Eq. (13) requires measurements of the inertial and relative position vectors. The benefit is that it is asymptotically stable. This simulation case shows the performance of the full-state feedback controller. The initial relative position vector of the two spacecraft system is

$$\boldsymbol{r}(t_0) = [4,\ 4,\ 0]^T \text{ m} \tag{55}$$

Note that while the Coulomb virtual structure literature discusses using electrostatic forces to compensate for differential gravity up to 100 meters at geosynchronous orbits, with the rotating system the separation distances are held to much smaller values. Otherwise, the rotational accelerations would require very large charge levels to compensate. As a comparison, the charged relative motion control discussion in Reference [18] considers stabilizing a two-craft system to a static equilibrium configuration over a day, while the present simulations are considering spin periods on the order of an hour. The initial relative velocity is

$$\dot{\boldsymbol{r}}(t_0) = [0.02,\ 0,\ 0.02]^T \text{ m/s} \tag{56}$$

The expected separation distance is $L^* = 4$m. The Debye length is $\lambda_d = 150$m. The two controller coefficients are

$$p = 1 \times 10^{-5}\text{s}^{-2}, \quad d = 4 \times 10^{-3}\text{s}^{-1} \tag{57}$$

Figure 5 shows the simulation results. Figure 5(a) shows the scenario as seen from the inertial frame centered at the CM of the two-craft system. The distance history in Figure 5(b) shows that the separation distance converges to the desired distance. Figure 5(c) shows the control charge product converges to the feed-forward charge product. Figure 5(d) shows the magnitude of the Coulomb force. During the simulation the Coulomb force is within 10mN.

B. Partial-State Feedback Simulation

This paper develops two partial-state feedback control law given by Eqs. (16) and (29). The control in Eq. (16) is stable assuming a fast spinning rate comparing to the GEO orbit rate. But when the estimation $\hat{f}_2$ is not equal to f_2^*, the separation distance would be biased to the expected distance. The control in Eq. (29) utilizes an integral feedback to compensate for the bias. But the stability is not proved.

The initial conditions and the control parameters are the same with the previous given by Eqs. (55)–(57). Figure 6 shows the simulation results using the feedback control law in Eq. (16). In this case the feed-forward part has the perfect guess of the f_2^* value. It can be seen that the distance converges

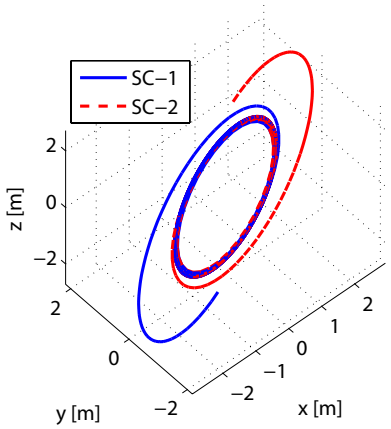

(a) Scenario seen from CM centered inertial frame.

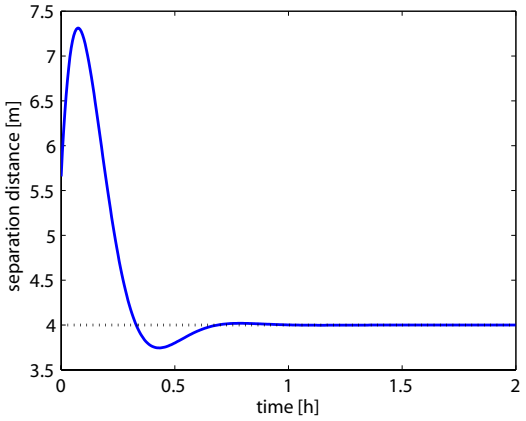

(b) Distance history.

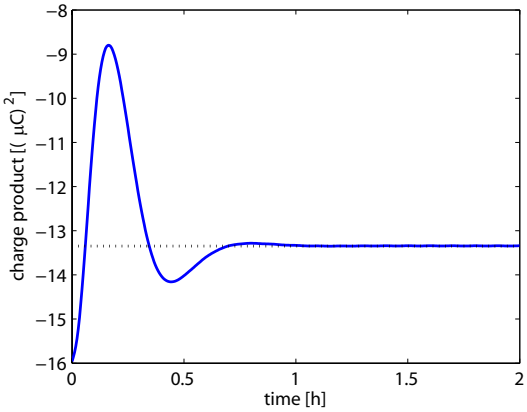

(c) Charge product.

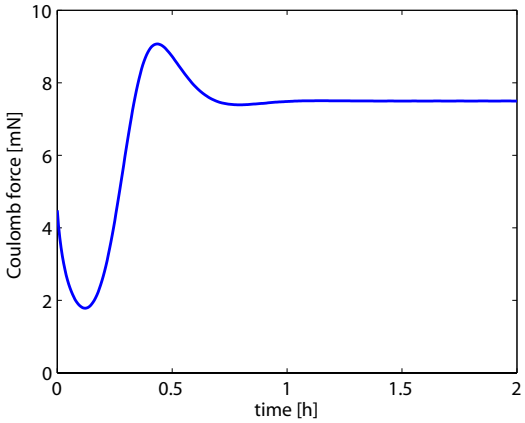

(d) Magnitude of the Coulomb force.

Fig. 5. Full-state feedback control law simulation.

to the expected distance and the charge product converges to the feed-forward charge product.

Figure 7 shows results of the same controller except that the estimation $\hat{f}_2$ is not equal to f_2^*. Figure 7 shows that there is a constant bias in the separation distance and the charge product. This control is stable, but it can not remove the constant bias.

Figure 8 shows simulation under the control in Eq. (29). The integral feedback coefficient is $k_i = 1 \times 10^{-7}\text{s}^{-3}$. The integral feedback term removes the constant biases in the separation distance and the charge product. This shows the great advantage of the integral feedback control law. But the stability of the feedback control law with the integral feedback is not proved analytically.

V. Conclusion

This paper investigates a two-craft Coulomb virtual structure control problem. A Lyapunov-based full-state feedback controller and a partial-state feedback controller are developed. The full-state feedback control law is asymptotically stable, but it requires measurements of the inertial and relative position vectors which may be challenging to obtain. The partial-state feedback control law without integral feedback is stable assuming a fast spinning rate in comparison to the orbit rate. But here the unmeasured states cause an estimation error of the relative position function in the feed-forward component which introduces a constant bias in the distance tracking error. An integral feedback term inserted into the partial-state feedback control law removes the constant bias. Numerical simulations illustrate the stability of using an integral feedback control law component. Note that the current control is specifically developed for a two spacecraft configuration. For larger clusters of craft there are additional control issues that must be addressed as the control now is non-affine in terms of the individual charges, and the mapping from charge products to charges can lead to imaginary solutions. In contrast, for the two-craft configuration we can determine the required single required charge product for which there is always a real individual charge solution.

References

[1] L. B. King, G. G. Parker, S. Deshmukh, and J.-H. Chong, "Spacecraft formation-flying using inter-vehicle coulomb forces," NASA/NIAC, Tech. Rep., January 2002, http://www.niac.usra.edu.

[2] J. H. Cover, W. Knauer, and H. A. Maurer, "Lightweight reflecting structures utilizing electrostatic inflation," US Patent 3,546,706, October 1966.

[3] E. M. C. Kong and D. W. Kwon, "Electromagnetic formation flight for multisatellite arrays," *Journal of Spacecraft and Rockets*, vol. 41, no. 4, July–Aug. 2004.

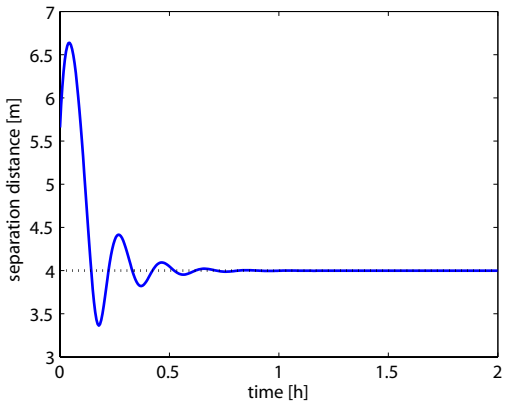

(a) Distance history.

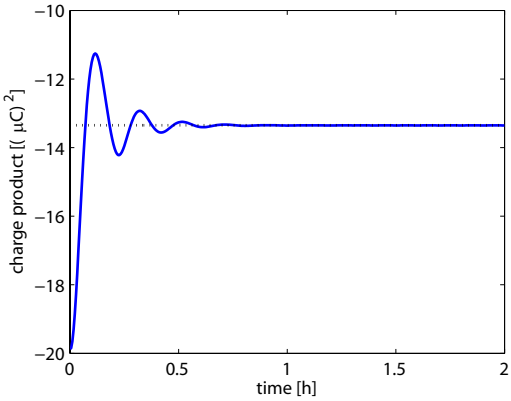

(b) Charge product.

Fig. 6. Partial-state feedback control law without integral feedback, with perfect estimation of f_2^*.

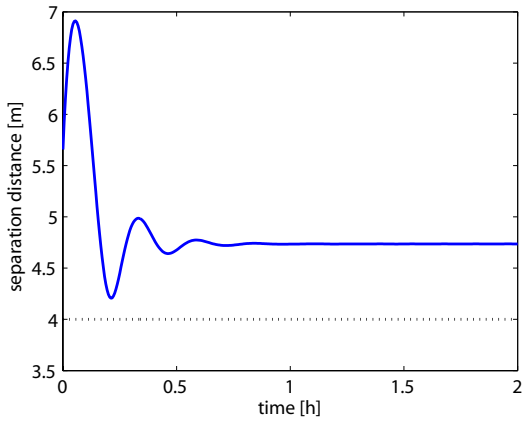

(a) Distance history.

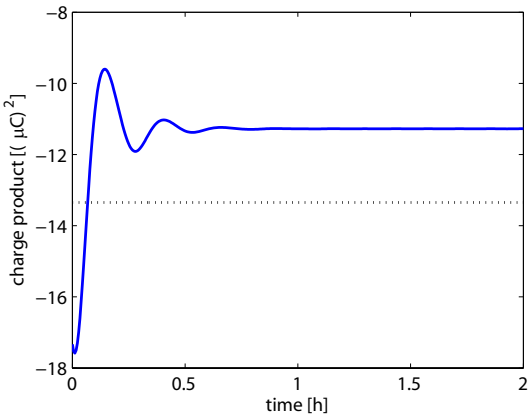

(b) Charge product.

Fig. 7. Partial-state feedback control law without integral feedback, $\hat{f}_2 = 0.81 f_2^*$.

[4] D. Scharf, F. Hadaegh, and S. Ploen, "A survey of spacecraft formation flying guidance and control (part II): control," in *Proceedings of the American Control Conference*, 2004, pp. 2976–2985.

[5] V. Kapila, A. G. Sparks, J. M. Buffington, and Q. Yan, "Spacecraft formation flying: Dynamics and control," in *Proceedings of the American Control Conference*, San Diego, California, June 1999, pp. 4137–4141.

[6] H. Schaub and K. T. Alfriend, "j_2 invariant relative orbits for spacecraft formations," *Celestial Mechanics and Dynamical Astronomy*, vol. 79, no. 2, pp. 77–95, 2001.

[7] L. B. King, G. G. Parker, S. Deshmukh, and J.-H. Chong, "Study of interspacecraft coulomb forces and implications for formation flying," *AIAA Journal of Propulsion and Power*, vol. 19, no. 3, pp. 497–505, May–June 2003.

[8] D. R. Nicholson, *Introduction to Plasma Theory*. Malabar, FL: Krieger, 1992.

[9] J. A. Bittencourt, *Fundamentals Of Plasma Physics*. Springer-Verlag New York, Inc., 175 Fifth Avenue, New York, NY, 2004.

[10] C. C. Romanelli, A. Natarajan, H. Schaub, G. G. Parker, and L. B. King, "Coulomb spacecraft voltage study due to differential orbital perturbations," in *AAS/AIAA Spaceflight Mechanics Meeting*, Tampa, FL, Jan. 22–26 2006, paper No. AAS-06-123.

[11] J. Berryman and H. Schaub, "Static equilibrium configurations in GEO coulomb spacecraft formations," in *AAS/AIAA Spaceflight Mechanics Meeting*, Copper Mountain, CO, Jan. 23–27 2005, paper No. AAS 05–104.

[12] ——, "Analytical charge analysis for 2- and 3-craft coulomb formations," *AIAA Journal of Guidance, Control, and Dynamics*, vol. 30, no. 6, pp. 1701–1710, Nov.–Dec. 2007.

[13] H. Schaub, C. Hall, and J. Berryman, "Necessary conditions for circularly-restricted static coulomb formations," *Journal of the Astronautical Sciences*, vol. 54, no. 3–4, pp. 525–541, July-Dec. 2006.

[14] H. Vasavada and H. Schaub, "Analytic solutions for equal mass four-craft static coulomb formation," *Journal of the Astronautical Sciences*, vol. 56, no. 1, pp. 7–40, Jan. – March 2008.

[15] A. Natarajan and H. Schaub, "Linear dynamics and stability analysis of a coulomb tether formation," *AIAA Journal of Guidance, Control, and Dynamics*, vol. 29, no. 4, pp. 831–839, July–Aug. 2006.

[16] ——, "Hybrid control of orbit normal and along-track two-craft coulomb tethers," *Aerospace Science and Technology*, vol. 13, no. 4–5, pp. 183–191, June–July 2009. [Online]. Available: http://dx.doi.org/doi:10.1016/j.ast.2008.10.002

[17] A. Natarajan, H. Schaub, and G. G. Parker, "Reconfiguration of a nadir-pointing 2-craft coulomb tether," *Journal of British Interplanetary Society*, vol. 60, no. 6, pp. 209–218, June 2007.

[18] A. Natarajan and H. Schaub, "Orbit-nadir aligned coulomb tether reconfiguration analysis," *Journal of the Astronautical Sciences*, vol. 56, no. 4, pp. 573–592, Oct. – Dec. 2008.

[19] H. Schaub and I. I. Hussein, "Stability and reconfiguration analysis of a circulary spinning 2-craft coulomb tether," in *IEEE Aerospace Conference*, Big Sky, MT, March 3–10 2007.

[20] I. I. Hussein and H. Schaub, "Stability and control of relative equilibria for the three-spacecraft coulomb tether problem," *Acta Astronautica*, vol. 65, no. 5–6, pp. 738–754, 2009.

[21] S. Wang and H. Schaub, "1-d constrained coulomb structure stabilization with charge saturation," in *AAS/AIAA Astrodynamics Specialist Conference*, Mackinac Island, MI, Aug. 19–23 2007, Paper AAS 07–267.

[22] H. Joe, H. Schaub, and G. G. Parker, "Formation dynamics of coulomb satellites," in *6th International Conference on Dynamics and Control of Systems and Structures in Space*, Riomaggiore, Cinque Terre, Italy, July 2004, pp. 79–90.

[23] V. J. Lappas, C. Saaj, D. J. Richie, M. A. Peck, B. Streetman, and H. Schaub, "Spacecraft formation flying and reconfiguration with electrostatic forces," in *AAS/AIAA Spaceflight Mechanics Meeting*, Sedona,

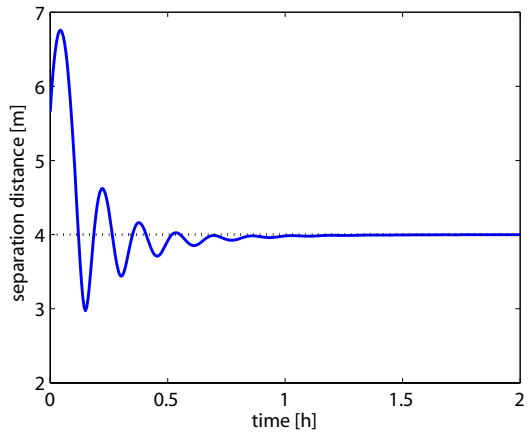

(a) Distance history.

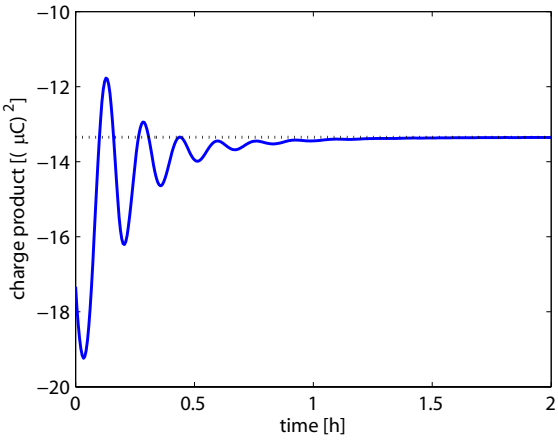

(b) Charge product.

Fig. 8. Partial-state feedback control law with integral feedback, $\hat{f}_2 = 0.81 f_2^*$.

AZ, Jan. 28–Feb. 1 2007, Paper AAS 07–113.

[24] G. Parker, H. Schaub, and K. Groom, "Tg3637 lumped parameter drive system dynamic model with speed and acceleration limits," Michigan Technological Univeristy, Tech. Rep., October 2000.

[25] S. Wang and H. Schaub, "Spacecraft collision avoidance using coulomb forces with separation distance feedback," *AIAA Journal of Guidance, Control, and Dynamics*, vol. 31, no. 3, pp. 740–750, May–June 2008.

[26] ——, "Electrostatic spacecraft collision avoidance using piece-wise constant charges," *AIAA Journal of Guidance, Control, and Dynamics*, vol. 33, no. 2, pp. 510–520, Mar.–Apr. 2010.

[27] R. Mukherjee and D. Chen, "Asymptotic stability theorem for autonomous systems," *AIAA Journal of Guidance, Control, and Dynamics*, vol. 16, pp. 961–963, Sept.–Oct. 1993.